Chemistry A European Journal

Chemistry Europe
European Chemical Societies Publishing

Title: Pathway-Dependent Phase Transitions of Supramolecular Self-Assemblies Containing Cationic Amphiphiles with Azobenzene and Disulfide Groups

Authors: Daichi Sawada, Kouichi Asakura, and Taisuke Banno

To be cited as: *Chem. Eur. J.* 10.1002/chem.202102143

Link to VoR: https://doi.org/10.1002/chem.202102143

WILEY-VCH

RESEARCH ARTICLE

Pathway-Dependent Phase Transitions of Supramolecular Self-Assemblies Containing Cationic Amphiphiles with Azobenzene and Disulfide Groups

Daichi Sawada,[a] Kouichi Asakura, [a] Taisuke Banno*[a]

[a] Daichi Sawada, Prof. Dr. Kouichi Asakura, Dr. Taisuke Banno
Department of Applied Chemistry, Faculty of Science and Technology
Keio University
3–14–1 Hiyoshi, Kohoku-ku, Yokohama 223–8522, JAPAN
E-mail: banno@applc.keio.ac.jp

Supporting information for this article is given via a link at the end of the document.

Abstract: There have been several attempts to construct supramolecular chemical systems that mimic the phase transitions in living systems. However, most of these phase transitions are one-to-one and induced by one stimulus or chemical; there have been few reports on the pathway-dependent phase transition of supramolecular self-assemblies in multi-step. To induce multistep phase transitions, we prepared molecular crystals containing a cationic amphiphile having azobenzene and disulfide groups. A reducing agent caused the crystals to become vesicles, and adjacent, non-touching vesicles fused under UV and subsequent visible light. Adding a reducing agent to the worm-like aggregates that were generated after UV irradiation of the original crystals resulted in the growth of sheet-like aggregates. ^{1}H NMR and fluorescence anisotropy measurements showed that a series of phase transitions was induced by changes in the phase structures from molecular conversions of the reactive amphiphiles. The multiple pathway-dependent phase transitions of supramolecular self-assemblies can provide a methodology for developing new stimuli-responsive materials that exhibit the desirable properties under specific circumstances from Systems Chemistry viewpoint.

Introduction

Phase transitions are essential for life. For example, cell membranes become harder or softer as a result of a temperature-dependent variation in amphiphile composition.[1] Liquid–liquid phase separation in the cytoplasm, which occurs through intermolecular interactions of the cytoplasm components, is also thought to be related to the maintenance of living systems.[2] Such behaviors are induced by complex hierarchical structures that range in size from angstroms to micrometers. In the last several decades, various supramolecular chemical systems have drawn considerable attention as living system-mimetic materials to induce the complex behaviors that lead to phase transitions.[3] Because of the dynamic and reversible nature of non-covalent interactions, supramolecular self-assemblies are stimuli-responsive with structural phase transitions that include dynamic behaviors, making them candidates for adaptive and smart materials.[4] For example, the fusion and fission of vesicles can be reversibly controlled by redox reactions using metal ions.[5] In addition, the phase transition from micelles to vesicles can be induced by a dehydrocondensation reaction to produce amphiphilic molecules.[6] Recently, in the field of systems chemistry, the continuous dynamic and transient structurization of supramolecular assemblies via molecular conversions of building blocks in the presence of polymerization initiators,[7] chemical catalysts,[8] enzymes,[9] or fuels[10] has been reported. The time-evolving formation process[11] and autocatalytic growth[12] of supramolecular assemblies have also been investigated. Reversibility in response to stimuli may lead to applications of self-assemblies as recyclable, degradable, and self-healing materials.[13] Despite the considerable progress made so far, most of the structural transitions are one-to-one and induced by one stimulus or chemical substance. Phase transitions with more than two steps would provide us with a new aspect to systems chemistry, which could be related to a pathway-dependent higher- or lower-ordering structurization.[14] Although multistep motion at the molecular level, such as unidirectional motion and rotation, by using precisely designed synthetic molecules has been reported,[15] it is still challenging to construct supramolecular chemical systems where macroscopic structures are successively transformed in conjunction with molecular conversions under multiple different stimuli.[16]

Herein, we report pathway-dependent phase transitions in supramolecular self-assemblies that respond to multiple stimuli. To construct such a supramolecular chemical system, we designed and synthesized a cationic amphiphile, **AzoSS**, which has azobenzene and disulfide groups (Figure 1a). Because there would be significant differences in the physicochemical properties between the reduced and isomerized products, it was expected that the application order of the stimuli would afford different supramolecular self-assemblies depending on the initial compositions, i.e., pathway-dependent phase transitions. We therefore investigated the effects of the application order of a reducing agent and UV irradiation (Paths 1 and 2 in Figure 1a) on the phase transition of the supramolecular assemblies.

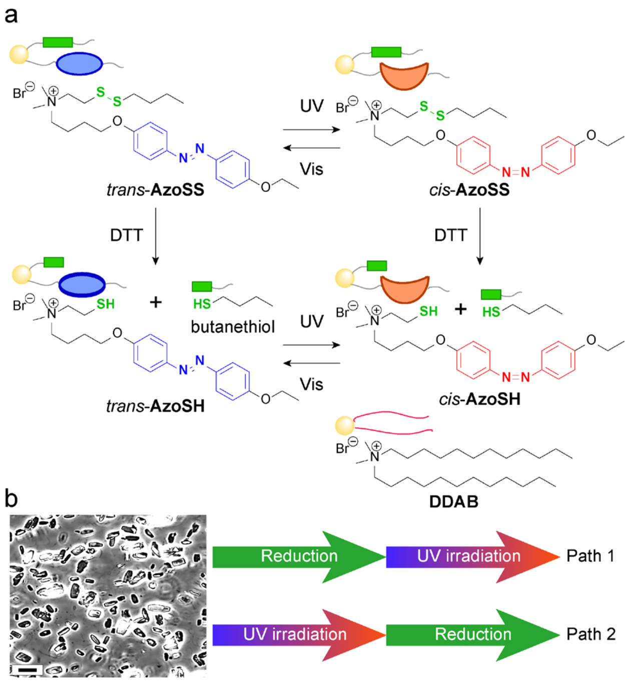

Figure 1. (a) Molecular structures of the cationic amphiphiles and reaction of **AzoSS** to the application of 1,4-dithiothreitol (DTT) and light. (b) Application of the stimuli to crystals composed of **AzoSS** and **DDAB** (80/20 mol/mol) shown in the micrograph by two different pathways. Scale bar: 10 mm.

Results and Discussion

Supramolecular assemblies were formed in a 1 mM dispersion of **AzoSS** and didodecyldimethylammonium bromide (**DDAB**) at ratios of 100/0, 80/20, 50/50, and 20/80 (mol/mol). We added the unreactive cationic amphiphile **DDAB** to the system because crystals composed of **AzoSS** dissolved when DTT was added. The hydrophobic fluorescent probe Nile red was added to the amphiphile dispersion to make the phase structures of the assemblies more visible under an optical microscope. Crystals with an interference in the cross-Nicol alignment were observed in the dispersion composed of **AzoSS**/**DDAB** = 80/20 (mol/mol) (Figure 1b). The supramolecular assemblies were first subjected to 1,4-dithiothreitol (DTT) followed by UV irradiation (Path 1). When DTT was added to the dispersion, aggregates with membrane structures formed from the surface of the crystals and enlarged while the crystals shrunk (Figure 2a). Since the hydrophobic Nile red was localized in the membranes, the generated structures were assumed to be vesicles. The phase transition from crystals to vesicles was further confirmed by image analysis using two different fluorescent probes: Nile red and BODIPY (Figures S1 and S2). Crystals were also observed at **AzoSS**/**DDAB** ratios of 50/50 and 20/80 (mol/mol); however, these crystals gradually shrunk and dissolved into the bulk solution when DTT was added. Therefore, 80 mol% **AzoSS** was used for further investigations into the mechanism of the phase transition from molecular crystals to vesicles.

Nile red is an environment-responsive probe whose maximum fluorescence wavelength changes depending on the surrounding polar environment,[17] which makes it useful for investigating the phase structures of various molecular self-assemblies.[18] In a **DDAB** dispersion, no fluorescence peak shift was observed after the addition of DTT (Figure S3). In contrast, a blue shift of the maximum fluorescence wavelength was observed for the 80/20 (mol/mol) **AzoSS**/**DDAB** dispersion in the presence of DTT (Figure 2b), suggesting that the localized environment of Nile red had changed after the addition of DTT. Because Nile red was added to the dispersion after the sample preparation, Nile red was not incorporated into the crystal but located in the crystal surface. This indicates that Nile red was exposed to the bulk aqueous phase, which is a highly polar environment, and its fluorescence intensity was relatively low. After the addition of DTT, Nile red was incorporated into the membrane, which has a lower polar environment, resulting in a blue shift of the maximum fluorescence wavelength with a higher intensity. In addition, the size distribution of nanometer-scale particles was measured by dynamic light scattering. A broad peak with a maximum number at 250 nm that was present in the dispersion without DTT became bimodal peaks with maxima at 800 and 100 nm after the addition of DTT. The peak at 800 nm slightly but steadily increased over time, implying the growth of vesicles (Figure 2c). Changes in the size distribution of assemblies at about 100 nm with time suggested that the submicrometer-sized structures proceeded to change during the observation period. Furthermore, ^{1}H NMR measurements were carried out to monitor the reduction ratio of the disulfide group in **AzoSS** and clarify the effect of the change in amphiphile composition on the phase transition from crystals to vesicles (Figure S4). Since the water solubilities of **AzoSS** and **DDAB** are quite low, it was assumed that the reaction mainly occurred at the surface of the crystals. Therefore, the concentrations of amphiphile and DTT were set to 10 mM and 40 mM, respectively, as one of a concentrated condition. As a result, the reduction of **AzoSS** to **AzoSH** gradually proceeded, and the reduction ratio was constant at ~65% within 10 min after the addition of DTT (Figure 2d). Therefore, the chemical composition of **AzoSS**, **AzoSH**, and **DDAB** was estimated to be 28/52/20 (mol/mol/mol). To investigate the effect of amphiphile composition on the formation of supramolecular assemblies, we observed the amphiphile dispersion at various molar ratios (Figure S5). Vesicles were clearly confirmed in the dispersions containing 40 or 60 mol% **AzoSH**. These results suggested that the phase transition from crystals to vesicles was induced by the reduction of **AzoSS** causing changes in phase structures based on the amphiphile composition.

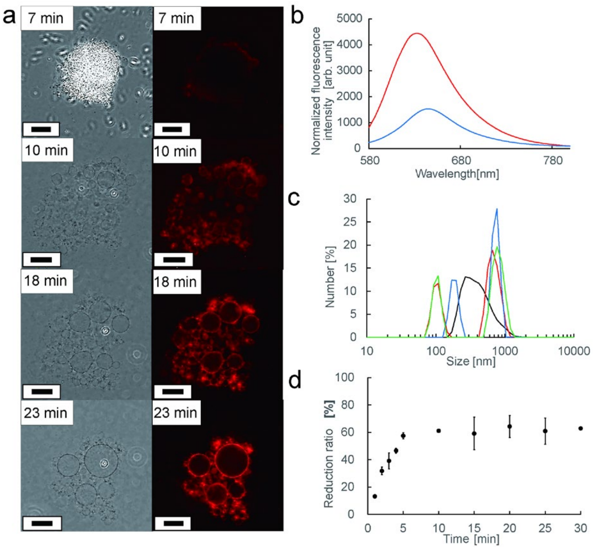

Figure 2. Phase transition from crystals to vesicles in a 1 mM dispersion of 80/20 (mol/mol) **AzoSS**/**DDAB** in the presence of DTT. (a) Sequential bright field and fluorescence images of the transformation from crystals to vesicles. l_{ex} = 559 nm and l_{em} = 570-670 nm for the fluorescence mode. Scale bar: 50 µm. (b) Fluorescence spectra of amphiphile dispersions containing Nile red before (blue) and after (red) the addition of 4 mM DTT. The spectra were normalized at the wavelength of 800 nm. (c) Particle size distribution in the dispersion before (black) and 10 min (red), 20 min (blue), and 30 min (green) after the addition of DTT by dynamic light scattering (d) Time-course of the reduction ratio of **AzoSS** by ^{1}H NMR analysis.

When a dispersion of 28/52/20 (mol/mol/mol) **AzoSS**/**AzoSH**/**DDAB** was irradiated with UV light, it could be seen under confocal laser scanning microscopy (CLSM) in the fluorescence mode that a part of the vesicle membrane disappeared and the vesicles fused together within 1 min by connecting their edges (Figure 3a and Movies S1 and S2). A similar fusion of vesicles was also observed under subsequent visible light irradiation (Figure S6). The photoisomerization ratio of the azobenzene-containing amphiphiles in D_2O when UV irradiation was applied to the dispersion after the reduction by DTT was monitored by ^{1}H NMR (Figure S7). The total amount of the *cis* isomer of azobenzene gradually increased over 10 min of UV irradiation. Under subsequent visible light irradiation, the amount of *cis*-isomer clearly decreased within 10 min (Figure 3b). The phase structures in the vesicular membrane under UV and visible light irradiation were evaluated by fluorescence anisotropy using Nile red[19] and BODIPY,[20] which are considered to be located inside and on the surface of the membrane, respectively. The fluidity parameter was calculated from $P = (I_{\parallel} - GI_{\perp})/(I_{\parallel} + GI_{\perp})$, where $I_{\perp}$, $I_{\parallel}$, $i_{\perp}$, and $i_{\parallel}$ are the emission intensities perpendicular and parallel to the vertically and horizontally polarized light, respectively, and G is the correction factor, $G = i_{\perp}/i_{\parallel}$. A larger $1/P$ value indicates higher fluidity in the vesicle membrane. The $1/P$ for BODIPY decreased slightly after DTT addition and subsequent UV irradiation, whereas that for Nile red decreased more significantly (Figure 3c). These results suggested that a significant difference in the fluidity between the inside of the vesicle and the membrane surface may induce instability in the phase structures, causing collapse of the local membrane which results in the vesicle having a micrometer-sized pore as a defect. Since the vesicles having such a defect were not thermodynamically stable,[21] when two vesicles were adjacent, they fused by connecting their edges. Under subsequent visible light irradiation, a similar instability in the phase structures, which led to the vesicle fusion, was also considered to be occurred from the result of fluorescence anisotropy (III in Figure 3c). The vesicle fusion was observed when the vesicles were close together under light irradiation. The Coulombic interaction based on the lipid species is one of dominant force for vesicle aggregation and fusion.[22] We thus carried out the measurement of ζ potential for the dispersions. The ζ potential became slightly larger after both DTT addition and UV irradiation (Figure 3d), indicating that Coulombic interactions were not the dominant force for vesicle fusion Therefore, the unusual fusion behavior of the vesicles was probably attributable to membrane instability induced by photoisomerization of the azobenzene compounds.

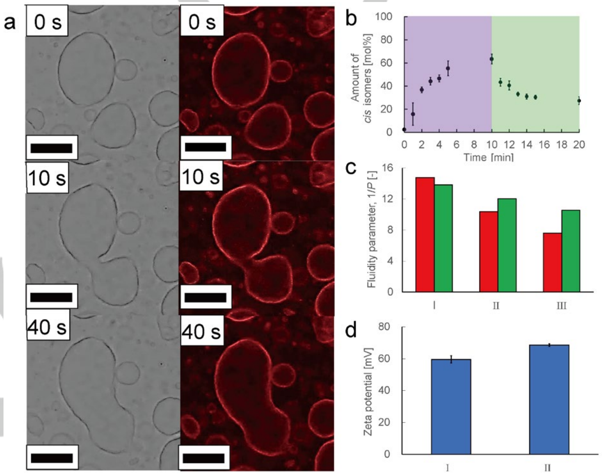

Figure 3. Fusion of vesicles under light irradiation after the addition of DTT to the 80/20 (mol/mol) **AzoSS**/**DDAB** dispersion. (a) Sequential bright field (left) and fluorescence (right) micrographs under UV irradiation. The fluorescence mode was the same as that for Fig. 2. Scale bar: 30 µm. (b) Time-course of the *cis*-isomer ratio after reduction by DTT (N = 3). The purple and green background colors indicate UV and visible light irradiation, respectively. (c) Fluidity parameter $1/P$ estimated by fluorescence anisotropy measurements of dispersions containing Nile red (red) and BODIPY (green). I: 30 min after the addition of DTT, II: 10 min after UV irradiation that was performed after step I, III: 10 min after visible light irradiation that was performed after step II. (d) Zeta potential of the dispersions (N = 3). I and II represent the same conditions as described in graph c.

Next, we observed the phase transition of the molecular self-assemblies in an 80/20 (mol/mol) **AzoSS**/**DDAB** dispersion following Path 2 (Figure 1b). When the dispersion was irradiated with UV light, the crystals in the irradiated area disappeared under microscope observation (Figure 4a). From the ^{1}H NMR analysis, the amount of *cis*-**AzoSS** significantly increased 30 min after UV irradiation (Figure S8). Since the melting point of *trans*-**AzoSS** was >200 °C according to differential scanning calorimetry, most crystals did not melt to a liquid but dissolved into the aqueous phase owing to the high solubility of *cis*-**AzoSS**. Under subsequent visible light irradiation, the crystals regenerated by reversible photoisomerization from the *cis* to the *trans* isomer (Figure S9).

By adding DTT after UV irradiation, the remaining worm-like aggregates gradually assembled to form larger sheet-like aggregates (Figure 4a). The reduction ratio of **AzoSS** after 30 min was determined to be 40% by ^{1}H NMR (Figure S10). Since the amount of butanethiol produced was estimated to be below its

10.1002/chem.202102143

solubility limit in water, butanethiol was unlikely to be the cause of the sheet-like aggregate formation, and we investigated the possible production of a hydrophobic component. Considering the interaction between thiol and quaternary ammonium, the dissociation of thiol group would be expected to occur more easily in a higher polar environment. Significant differences in the ^{1}H NMR spectrum of **AzoSH** were observed depending on the NMR solvent composition used. The methylene group in the vicinity of thiol group was detected at 2.93 ppm in CD_3OD, whereas a part of that peak appeared at a lower field of 3.68 ppm in a mixed D_2O/CD_3OD solvent (Figure 4c). In the ^{1}H-^{1}H COSY spectrum of **AzoSH** using a mixed solvent, a clear correlation between the methylene group in the vicinity of quaternary ammonium (*d* 3.15 ppm) and thiol groups (*d* 3.68 ppm) was also confirmed (Figure S11), indicating that these functional groups interacted. In addition, dissociation of the thiol group may occur in the highly hydrophilic environment owing to the relatively strong acidity of the thiol group. This suggested the production of cation–anion pair. In the presence of 1 mM NaCl, no growth to sheet-like aggregates was observed (Figure S12). These results suggested that the interaction between the quaternary ammonium cations and the thiol group (and thiolate anions) was essential for growth to sheet-like aggregates. Therefore, it was considered that the formation and growth of sheet-like aggregates was induced by hydrophobic interactions owing to electrostatic shielding of the quaternary ammonium groups.

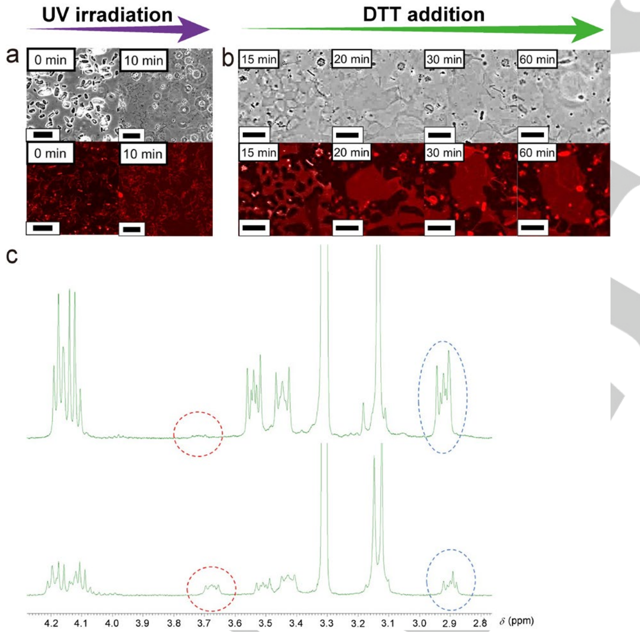

Figure 4. Phase transition of supramolecular self-assemblies in the 80/20 (mol/mol) **AzoSS/DDAB** dispersion by applying UV irradiation and DTT. (a) Bright field (top) and fluorescence (bottom) images before and after UV irradiation. Scale bar: 30 μm. (b) Bright field (top) and fluorescence (bottom) images of aggregate growth after 10 min UV irradiation followed by 4 mM DTT addition. Scale bar: 100 μm. The fluorescence mode was same as that in Fig. 2. (c) ^{1}H NMR spectra of **AzoSH** in CD_3OD (top) and 2/1 (v/v) CD_3OD/D_2O (bottom).

From the above results, the mechanism for the different pathway-dependent phase transitions was interpreted as follows. In the **DDAB** dispersion, no transformation occurred from crystals to other aggregates, indicating that the observed phase transitions were triggered by molecular conversions of **AzoSS**. Although crystals composed of **AzoSS** and **DDAB** had a relatively high orientation, neither the hydrophilic nor the hydrophobic groups were completely oriented in an orderly manner (Figure 5a). By adding DTT, the crystals transformed to vesicles having bilayer structures, indicating spontaneous rearrangement of the molecules through the reduction of **AzoSS** to produce **AzoSH** and butanethiol. This probably resulted from a decrease in the molecular packing that was based on the intermolecular interactions of **AzoSS**, **AzoSH** and **DDAB** (Figure 5b).[23] The isomerization that occurred under both UV and the subsequent visible light irradiation generated instability that led to the local collapse of vesicular membranes, inducing the vesicle fusion of two adjacent vesicles (Figure 5c). In contrast, when UV irradiation was applied first, most of the crystals that were composed of **AzoSS** and **DDAB** were soluble in the aqueous phase as a result of photoisomerization from the less soluble *trans* isomer to the more soluble *cis* isomer (Figure 5d). By subsequently adding DTT, the aggregation of building blocks led to the formation of sheet-like aggregates which grew as a result of the hydrophobic interactions of the components (Figure 5e). Thus, a molecular system composed of both azobenzene and disulfide provides a strategy for constructing supramolecular self-assemblies that exhibit multiple, pathway-dependent phase transitions. These findings may also provide insight into the emergence of life.[24] Although our chemical system consists of synthetic compounds, vesicles can be considered as models for cells,[25] and therefore the designed molecular system suggests one possibility for the chemical evolution of protocells that can generate in circumstances where various stimuli are applied.

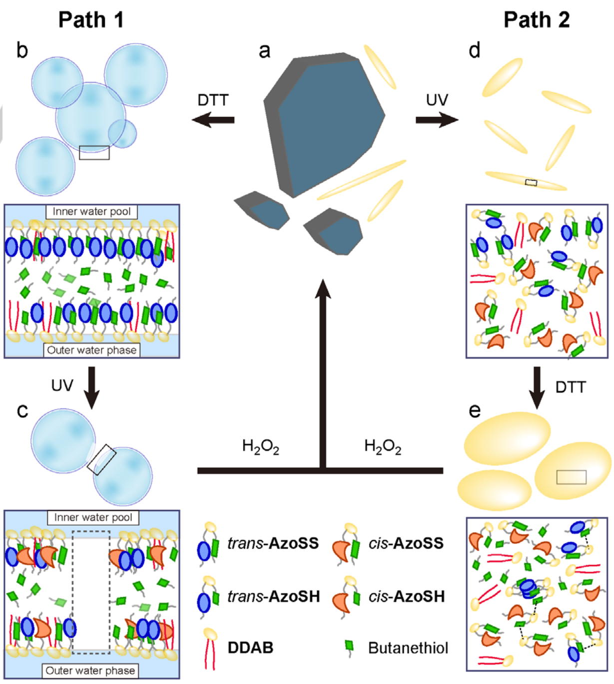

Figure 5. Schematic illustration of the phase transitions via Paths 1 and 2. a) Crystals composed of **AzoSS** and **DDAB**. b) Emergence of vesicles in the presence of DTT. c) Pore formation at the vesicular membrane indicated by the dotted square under UV irradiation. (d) Transformation to worm-like aggregates under UV irradiation. e) Formation and growth of sheet-like aggregates in the presence of DTT. Dashed lines indicate interactions between the quaternary ammonium cation and the thiol group.

Finally, we examined the reverse process of the phase transitions by adding H_2O_2 to the dispersions formed at the completion of each path. When 5 mM H_2O_2 solution was employed at the end of Path 1, the vesicles shrank and then the regeneration of crystals was observed under both CLSM and a polarizing optical microscope (Figure S13). A reversible transition between crystals and vesicles was repeatedly observed by adding DTT and H_2O_2 in turn (Figure S14). For Path 2, the sheet-like aggregates transformed to worm-like aggregates and eventually crystals by adding H_2O_2 at the end of the path (Figure S15). ^{1}H NMR showed both hetero- and homo-disulfide compounds (Figure S16); however, it was not possible to clearly estimate the precise composition. Furthermore, in the dispersion containing Nile red, a red shift was observed in the fluorescence spectra after the addition of H_2O_2 (Figure S17), suggesting that Nile red was located in a lower polar environment before the addition of H_2O_2 and a higher polar environment after the addition of H_2O_2. On the basis of these results, we considered that though the mechanism is not fully understood, the reversible phase transition was triggered by changes in the phase structures based on the redox reaction of **AzoSS** in both Paths 1 and 2. The pathway-independent reversibility indicates robustness as a chemical system, and could be an important factor for developing new stimuli-responsive materials[26] exhibiting desirable properties under specific circumstances.

Conclusion

We have demonstrated multiple pathway-dependent phase transitions of supramolecular self-assemblies by using cationic amphiphiles with azobenzene and disulfide groups. The original molecular crystals showed different phase transitions depending on the application order of a reduction agent and light irradiation. Applying a reduction agent first afforded a phase transition from crystals to vesicles, which fused without initially contacting each other under subsequent UV and visible light irradiation. In contrast, applying UV light to the original molecular crystals caused the formation of worm-like aggregates that then grew to sheet-like aggregates by the addition of a reducing agent. In addition, the phase change between crystals and vesicles or aggregates was reversible for both paths by a redox reaction. These phase transitions were induced by changes in the phase structures based on molecular conversions. The current molecular system can not only provide a methodology for developing new stimuli-responsive materials that exhibit the desirable properties under specific circumstances, but may also demonstrate a possible pathway in the chemical evolution of protocells, especially selection, from a Systems Chemistry viewpoint.

Acknowledgements

Mr. Tsuneyoshi Torii and Ms. Mitsuyo Matsubara (Malvern Panalytical, a division of Spectris Co. Ltd.) is acknowledged for the measurements of z potentials. We would like to thank Editage (www.editage.com) for English language editing. This work was supported by JSPS KAKENHI Grant Number 18K05066 for T.B.

Keywords: aggregation • amphiphiles • phase transitions • self-assembly • vesicles

[1] J. R. Hazel, *Annu. Rev. Physiol.* **1995**, *57*, 19-42.

[2] a) P. A. Chong, J. D. Forman-Kay, *Curr. Opin. Struct.* **2016**, *41*, 180-186; b) A. A. Hyman, C. A. Weber, F. Julicher, *Annu. Rev. Cell Dev. Biol.* **2014**, *30*, 39-58.

[3] B. A. Grzybowski, K. Fitzner, J. Paczesny, S. Granick, *Chem. Soc. Rev.* **2017**, *46*, 5647-5678.

[4] a) G. M. Whitesides, B. Grzybowski, *Science* **2002**, *295*, 2418-2421; b) T. Aida, E. W. Meijer, S. I. Stupp, *Science* **2012**, *335*, 813-817.

[5] J. Li, K. Peng, Y. Li, J. Wang, J. Huang, Y. Yan, D. Wang, B. Z. Tang, *Angew. Chem. Int. Ed.* **2020**, *59*, 21510-21514; *Angew. Chem.* **2020**, *132*, 21694-21698.

[6] T. Toyota, K. Takakura, J. Kose, T. Sugawara, *ChemPhysChem* **2006**, *7*, 1425-1427.

[7] a) A. Blanazs, J. Madsen, G. Battaglia, A. J. Ryan, S. P. Armes, *J. Am. Chem. Soc.* **2011**, *133*, 16581-16587; b) X. Luo, S. Zhao, Y. Chen, L. Zhang, J. Tan, *Macromolecules* **2021**, *54*, 2948-2959; c) Q. Zhang, R. Zeng, Y. Zhang, Y. Chen, L. Zhang, J. Tan, *Macromolecules* **2020**, *53*, 8982-8991.

[8] a) K. Takakura, T. Yamamoto, K. Kurihara, T. Toyota, K. Ohnuma, T. Sugawara, *Chem. Commun.* **2014**, *50*, 2190-2192; b) T. Banno, Y. Tanaka, K. Asakura, T. Toyota, *Langmuir* **2016**, *32*, 9591-9597.

[9] a) S. Debnath, S. Roy, R. V. Ulijn, *J. Am. Chem. Soc.* **2013**, *135*, 16789 -16792; b) C. G. Pappas, I. R. Sasselli, R. V. Ulijn, *Angew. Chem. Int. Ed.* **2015**, *54*, 8119-8123; *Angew. Chem.* **2015**, *127*, 8237-8241.

[10] a) J. Boekhoven, A. M. Brizard, K. N. K. Kowlgi, G. J. M. Koper, R. Eelkema and J. H. van Esch, *Angew. Chem. Int. Ed.* **2010**, *49*, 4825-4828; *Angew. Chem.* **2010**, *122*, 4935-4938; b) J. Boekhoven, W. E. Hendriksen, G. J. M. Koper, R. Eelkema, J. H. van Esch, *Science* **2015**, *349*, 1075-1079; c) S. Maiti, I. Fortunati, C. Ferrante, P. Scrimin, L. J. Prins, *Nat. Chem.* **2016**, *8*, 725-731.

[11] a) P. Jonkheijm, P. Schoot, A. P. H. J. Schenning, E. W. Meijer, *Science* **2006**, *313*, 80-83; b) P. A. Korevaar, S. J. George, A. J. Markvoort, M. M. J. Smulders, P. A. J. Hilbers, A. P. H. J. Schenning, T. F. A. De Greef, E. W. Meijer, *Nature* **2012**, *481*, 492-495.

[12] a) J. M. A. Carnall, C. A. Waudby, A. M. Belenguer, M. C. A. Stuart, J. Peyralans, S. Otto, *Science* **2010**, *327*, 1502-1506; b) Y. Altay, M. Tezcan, S. Otto, *J. Am. Chem. Soc.* **2017**, *139*, 13612-13615.

[13] a) X. Yan, F. Wang, B. Zheng, F. Huang, *Chem. Soc. Rev.* **2012**, *41*, 6042-6065; b) L. Yang, X. Tan, Z. Wang, X. Zhang, *Chem. Rev.* **2015**, *115*, 7196-7239.

[14] S. A. P. van Rossum, M. Tena–Solsona, J. H. van Esch, R. Eelkema, J. Boekhoven, *Chem. Soc. Rev.* **2017**, *46*, 5519-5535.

[15] S. Kassem, T. van Leeuwen, A. S. Lubbe, M. R. Wilson, B. L. Feringa, D. A. Leigh, *Chem. Soc. Rev.* **2017**, *46*, 2592-2621.

[16] X. Yan, D. Xu, X. Chi, J. Chen, S. Dong, X. Ding, Y. Yu, F. Huang, *Adv. Mater.*, **2012**, *24*, 362-369.

[17] a) P. Greenspan, S. D. Fowler, *J. Lipid Res.* **1985**, *26*, 781-789; b) O. A. Kucherak, S. Oncul, Z. Darwich, D. A. Yushchenko, Y. Arntz, P. Didier, Y. Mély, A. S. Klymchenko, *J. Am. Chem. Soc.* **2010**, *132*, 4907-4916.

[18] a) I. N. Kurniasih, H. Liang, P. C. Mohr, G. Khot, J. P. Rabe, A. Mohr, *Langmuir* **2015**, *31*, 2639-2648; b) J. Mishra, A. K. Mishra, *Langmuir* **2018**, *34*, 11886-11897; c) M. C. A. Stuart, J. C. van de Pas, J. B. F. N. Engberts, *J. Phys. Org. Chem.* **2005**, *18*, 929-934; d) J. Swain, A. K. Mishra, *Photochem. Photobiol. Sci.* **2016**, *15*, 1400-1407.

[19] a) S. Mukherjee, H. Raghuraman, A. Chattopadhyay, *Biochim. Biophys. Acta.* **2007**, *1768*, 59-66; b) E. Feitosa, F. R. Alves, A. Niemiec, M. E. C. D. R. Oliveira, E. M. S. Castanheira, A. L. F. Baptista, *Langmuir* **2006**, *22*, 3579-3585.

[20] a) M. Bacalum, L. Wang, S. Boodts, P. Yuan, V. Leen, N. Smisdom, E. Fron, S. Knippenberg, G. Fabre, P. Trouillas, D. Beljonne, W. Dehaen, N. Boens, M. Ameloot, *Langmuir* **2016**, *32*, 3495-3505; b) J. A. Levitt, P. Chung, M. K. Kuimova, G. Yahioglu, Y. Wang, J. Qu, K. Suhling, *Chem PhysChem* **2011**, *12*, 662-672.

[21] a) T. Hamada, R. Sugimoto, M. C. Vestergaard, T. Nagasaki, M. Takagi, *J. Am. Chem. Soc.* **2010**, *132*, 10528-10532; b) R. B. Lira, F. S. C. Leomil,

10.1002/chem.202102143

R. J. Melo, K. A. Riske, R. Dimova, *Adv. Sci.* **2020**, 2004068; c) F. Nomura, M. Nagata, T. Inaba, H. Hiramatsu, H. Hotani, K. Takiguchi, *Proc. Natl. Acad. Sci. U.S.A.* **2001**, *98*, 2340-2345; d) Y. Sakuma, T. Taniguchi, M. Imai, *Biophys. J.* **2010**, *99*, 472-479.

[22] a) J. Sawayama, H. Sakaino, S. Kabashima, I. Yoshikawa, K. Araki, *Langmuir* **2011**, *27*, 8653-8658; b) M. Mora, F. Mir, M. A. de Madariaga, M. L. Sagristá, *Lipids* **2000**, *35*, 513-524; c) K. Yasuhara, M, Tsukamoto, Y. Tsuji, J. Kikuchi, *Colloids Surf. A* **2012**, *415*, 461-467.

[23] a) M. Tameyuki, H. Hiranaka, T. Toyota, K. Asakura, T. Banno, *Langmuir* **2019**, *35*, 17075-17081; b) D. Sawada, A. Hirono, K. Asakura, T. Banno, *RSC Adv.* **2020**, *10*, 34247-34253.

[24] P. L. Luisi, in *The Emergence of Life: From Chemical Origins to Synthetic Biology*, Cambridge University Press, Cambridge, **2006**.

[25] a) P. L. Luisi, P. Walde, T. Oberholzer, *Curr. Opin. Colloid Interface Sci.* **1999**, *4*, 33-39; b) J. W. Szostak, D. P. Bartel, P. L. Luisi, *Nature* **2001**, *409*, 387-390.

[26] E. Mattia, S. Otto, *Nat. Nanotech.* **2015**, *10*, 111-119.

Entry for the Table of Contents

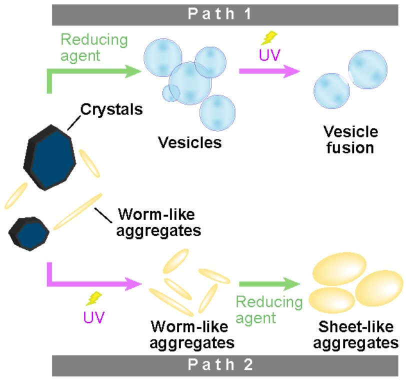

The original molecular crystals containing cationic amphiphiles with azobenzene and disulfide groups showed different phase transitions depending on the application order of a reduction agent and light irradiation. The current molecular system can provide a methodology for developing new stimuli-responsive materials that exhibit the desirable properties under specific circumstances from Systems Chemistry viewpoint.